

## Doping and temperature dependence of $c$ -axis optical phonons in $\text{YBa}_2\text{Cu}_3\text{O}_y$ single crystals

J. Schützmann, S. Tajima, S. Miyamoto, Y. Sato, and R. Hauff

*Superconductivity Research Laboratory, International Superconductivity Technology Center, Shinonome 1-10-13, Koto-ku, Tokyo 13, Japan*

(Received 4 May 1995)

Measuring the far-infrared reflectivity of  $\text{YBa}_2\text{Cu}_3\text{O}_y$  crystals with radiation polarized parallel to the  $c$  axis, we determined the doping and temperature dependence of  $c$ -axis infrared active phonons. Superconductivity related effects on the phonon self-energies are weak for the overdoped crystal, but pronounced for the optimally doped crystal. The differences are attributed to a lower symmetry of the optimally doped crystal due to disorder in the oxygen sublattice which manifests in a splitting of the apical oxygen vibration into well distinct modes above  $600\text{ cm}^{-1}$ . For the underdoped crystals anomalies are observed well above  $T_c$ . The onset temperature of the anomalies increases with decreasing doping, suggesting a relationship with the spin-gap temperature. The dramatic decrease in oscillator strength of the in-plane oxygen bending mode is related to a growth of a new broad excitation centered between  $450$  and  $400\text{ cm}^{-1}$ .

### I. INTRODUCTION

From the early stage of the research on high- $T_c$  superconductors the coupling of phonons to the electronic system has been an interesting issue. Differences in the real and imaginary parts of the phonon self-energies, obtained by Raman spectroscopy, have been applied to determine the superconducting energy gap<sup>1</sup> because even Raman modes should couple to the electronic background. Principally, odd infrared-active phonons may only couple with odd excitations like charge fluctuations between different  $\text{CuO}_2$  layers, i.e., between symmetric and antisymmetric bands. The influence of interband transitions on infrared-active phonons was calculated in Ref. 2 where a rapid change of the oscillator strengths at  $T_c$  was predicted.

A recent report<sup>3</sup> on anisotropic dc resistivity data suggested a strong relation between the in- and out-of-plane temperature dependence in the framework of a spin-charge separation picture. A similar picture was applied to interpret the infrared  $c$ -axis response where a gaplike structure is observed for underdoped  $\text{YBa}_2\text{Cu}_3\text{O}_y$  crystals<sup>4</sup> and  $\text{YBa}_2\text{Cu}_4\text{O}_8$  crystals.<sup>5</sup> On the other hand, it is suggested that this gaplike structure indicates a charge transfer between adjacent  $\text{CuO}_2$  planes.<sup>6</sup> Additionally, it is proposed that the  $c$ -axis charge transport is governed by interbilayer coupling which varies exponentially with doping due to changes of the  $\text{O}(4)\text{-Cu}(2)$  bond length and that  $c$ -axis phonons may contribute to phonon-assisted interlayer hopping in underdoped  $\text{YBa}_2\text{Cu}_3\text{O}_y$ .<sup>7</sup> Therefore, it is of interest to determine the doping and temperature dependence of phonons with respect to charge and spin excitations.

In the past, infrared-active phonons with eigenvectors parallel to the  $c$  axis of high-temperature superconductors were mainly studied in ceramic samples<sup>8-12</sup> due to the lack of crystals with sufficient  $c$ -axis dimensions. A serious problem had been the huge oscillator strengths which were found in the infrared conductivities derived from a Kramers-Kronig analysis of reflectivity data of these polycrystalline samples.

This is partly related to the fact that in frequency regions where the wavelength of the incident light is large compared to the typical dimensions of the crystallites ( $1\text{--}10\text{ }\mu\text{m}$ ) with different orientations of the  $c$  axis relative to the surface, the reflectivity is determined by a superposition of the corresponding conductivities. For wavelengths shorter than the average size of the crystallites the reflectivity is composed by the reflectivity of the different grains. Changes of the absolute reflectivity caused by a strong temperature dependence of the in-plane response may result in an artificial temperature dependence of the oscillator strength that is discussed more deeply in Ref. 13. Only few measurements were performed on single crystals<sup>4,14-17</sup> or a mosaic of them.<sup>18,19</sup> However, until now no consequent characterization of the different phonon modes with respect to their doping and temperature dependences have been carried out.

In this work we have measured the reflectivity of  $\text{YBa}_2\text{Cu}_3\text{O}_y$  with the electric-field vector  $\mathbf{E}$  polarized parallel to the  $c$ -axis of crystals with oxygen content of  $y \approx 6.1, 6.5, 6.6, 6.8,$  and  $6.9$  in a frequency range of  $30\text{--}10\,000\text{ cm}^{-1}$  and for temperatures between  $10$  and  $300\text{ K}$ . The infrared-active phonons have been analyzed by calculating the optical conductivity via a Kramers-Kronig transformation. For the crystals with highest oxygen content, which is overdoped, we found that the phonon parameters (resonance frequency, oscillator strength, and damping) are almost not affected by the superconducting transition except for a weak softening of the bending mode of the planar oxygen at  $315\text{ cm}^{-1}$  and a slight decrease of the linewidth of the Y mode at  $194\text{ cm}^{-1}$ . The oscillator strengths remain essentially unchanged in contrast to previous reports on ceramic samples.<sup>10</sup> In the case of almost optimal doping ( $y \approx 6.8$ ) the softening of the  $315\text{ cm}^{-1}$  is more pronounced and its strength rapidly drops at  $T_c$ . In addition the linewidths of phonons with resonance frequencies below  $320\text{ cm}^{-1}$  narrow whereas the two high-frequency phonons exhibit broadening just below  $T_c$  followed by a narrowing with further reducing temperature. For the highly reduced crystals a strong de-

crease of the resonance frequency of the in-plane oxygen modes is observed which sets in at  $\approx 100$  K for  $y \approx 6.6$  and  $\approx 160$  K for  $y \approx 6.5$ . At the same temperatures the corresponding oscillator strengths start to decrease. The spectral weight seems to be partly transferred to a broad absorption band in the vicinity of  $450$  and  $400$   $\text{cm}^{-1}$ , respectively.

## II. EXPERIMENT

The single crystals used in this study were cut from a large  $\text{YBa}_2\text{Cu}_3\text{O}_y$  crystal grown by a modified top-seeded pulling technique named solute-rich liquid-crystal pulling (SRLCP) method. We used as crucible material yttria and a  $\text{YBa}_2\text{Cu}_3\text{O}_y$  crystal as a seed, further details are published elsewhere.<sup>20</sup> Typical sizes of these crystals are 1 cm along each principle axis and they are therefore predestined for investigations especially of  $c$ -axis properties in contrast to flux samples with  $c$ -axis dimensions of only several hundreds  $\mu\text{m}$ . To obtain ac surfaces we cut several pieces (8 mm perpendicular and 5 mm parallel to the  $c$  axis) from the as-grown crystal and controlled the orientation by x-ray Laue backscattering. Before the annealing processes the amount of impurities was estimated by ICP mass spectroscopy to be less than 0.01 wt. % for metal impurities as Zn, Al, Ag, Au, and K. However, a small amount of Ca was detected ( $<0.2\%$ ) which could substitute for Y and act as acceptor, i.e., dope holes into the  $\text{CuO}_2$  planes.

Our as-grown crystals exhibit a broad superconductivity transition around 60 K and the further heat treatment was performed in the following way. One group of crystals was annealed at  $400$  °C in flowing oxygen for one month. Two other groups of crystals were sealed together with  $\text{YBa}_2\text{Cu}_3\text{O}_y$  polycrystalline powder in evacuated quartz tubes, which had been annealed at 480, 605, and 650 °C and quenched to room temperature before. The sealed crystals were then annealed for 10 days at 550 °C and at 600 °C in the case of the powder quenched from 650 °C. The resulting oxygen content of the crystals was determined by the results of iodometric measurements performed on the polycrystalline powder and to be  $y \approx 6.9$ , 6.8, 6.6, and 6.5, respectively. The oxygen content of another crystal was reduced to  $y \approx 6.1$  in 1 atmosphere flowing argon at 600 °C for 7 days.

The corresponding transition temperatures were determined by ac susceptibility measurements using a field of 0.02 Oe at a frequency of 1000 Hz. Taking into account demagnetization factors with respect to the sample shapes of the four superconducting crystals, we obtain magnetic shielding results displayed in Fig. 1. The crystal with highest oxygen content ( $y \approx 6.9$ ) showed a slightly reduced  $T_c \approx 88$  K compared to the almost optimally doped one ( $y \approx 6.8$ ) as a consequence of overdoping. We studied carefully the influence of annealing conditions on  $T_c$  and dc resistivity on a batch of several crystals cut from the same large crystal mentioned above.<sup>21</sup> We found that the optimal annealing temperature is 500 °C, leading to a  $T_c$  of 93 K, and that lowering the annealing temperature decreases  $T_c$  down to 88 K. This is accompanied by a decrease of the in-plane dc resistivity [ $\rho_{ab}(100 \text{ K}) \approx 25 \mu\Omega \text{ cm}$ ] and a change of its temperature dependence from linear to super linear with  $\rho_{ab} \propto T^\alpha$ ,  $1 < \alpha < 2$  suggestive for a change to a Fermi-liquid-like behavior. Moreover a negative in-plane Seebeck coefficient and

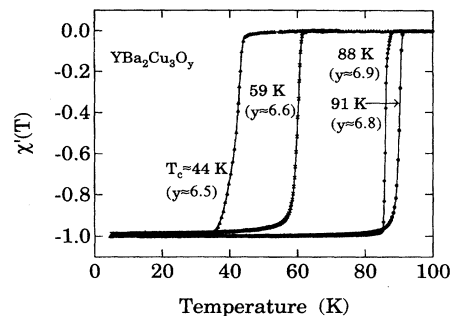


FIG. 1. Magnetic susceptibility of  $\text{YBa}_2\text{Cu}_3\text{O}_y$  ( $y \approx 6.9$ , 6.8, 6.6, and 6.5) single crystals. The measurements are performed with the magnetic field  $\mathbf{H} \parallel c$  ( $H = 20$  mOe,  $\omega = 1$  kHz).

small Hall resistivities confirm that these crystals are overdoped.<sup>22</sup> We note that we also checked the amount of impurities after the annealing processes and found no contamination. All crystals were polished prior to the optical measurements using  $\text{Al}_2\text{O}_3$  powder.

The infrared reflectivity measurements were performed with a fast-scan Fourier transform spectrometer (Bruker IFS 113V) and a helium-flow cryostat. The infrared radiation was polarized parallel to the  $c$  axis of the crystals ( $\mathbf{E} \parallel c$ ) by using wire grids on polyethylene and KRS5 substrates as well as a quartz polarizer for the appropriate frequency ranges ( $30$ – $10\,000$   $\text{cm}^{-1}$ ). Sample and reference spectra were measured immediately one after the other by exchanging sample and reference mirror (Au evaporated on a glass plate) and controlling their position relative to the incident infrared radiation with the light of a helium-neon Laser during the measurement. Taking advantage of the low pressure within the spectrometer we used very thin cryostat windows in the far-infrared frequency range (polyethylene with thickness  $\approx 50$   $\mu\text{m}$ ) and could therefore watch the position of sample and reference. We used a spot of the infrared beam on the sample that was smaller than the sample size itself, with the advantage that no further corrections regarding the shape of the sample were necessary. But, due to thermal shrinking of parts of the sample chamber and holder (up to 3 mm) the sample moves out of the focus which could be compensated by adjusting the position of the sample at each temperature. Temperature of the sample was precisely controlled by using helium exchange gas in the sample chamber. With this technique the overlap of the reflectivity spectra between  $500$  and  $650$   $\text{cm}^{-1}$  measured in the far-infrared and mid-infrared configuration was better than  $\pm 1\%$  that corresponds to our estimated accuracy of  $\pm 1\%$  in the absolute reflectivity. Between  $10\,000$  and  $33\,000$   $\text{cm}^{-1}$  reflectivity measurements were performed with a grating type spectrometer at room temperature.

## III. RESULTS AND ANALYSIS

### A. Reflectivity

The development of the  $c$ -axis reflectivity of  $\text{YBa}_2\text{Cu}_3\text{O}_y$  with increasing doping is shown in Fig. 2. There are two distinct features in the case of the superconducting crystals [Figs. 2(a)–2(d)]. One is the electronic background

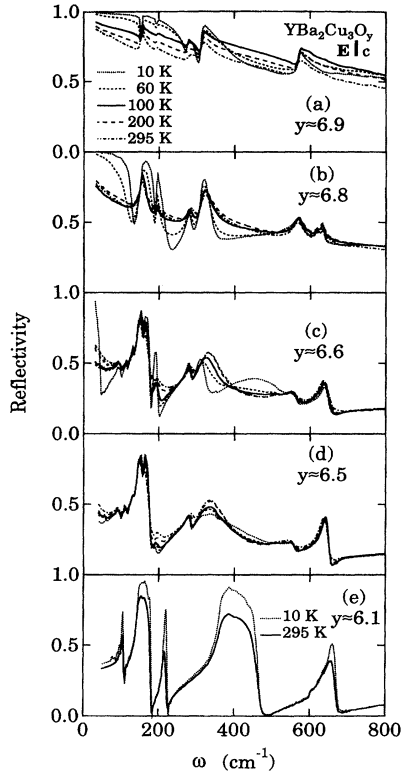


FIG. 2. Reflectivity of  $\text{YBa}_2\text{Cu}_3\text{O}_y$  crystals for  $y \approx 6.9$  (a) 6.8 (b), 6.6 (c), 6.5 (d), and 6.1 (e) measured with the electric field vector  $\mathbf{E} \parallel c$  at 295 K (dash-dotted curves), 200 K (dashed), 100 K (solid), 60 K (short-dashed), and 10 K (dotted).

reflectivity and the other is the response of infrared-active phonons. With increasing doping the background reflectivity increases and finally exhibits a metallic temperature dependence.<sup>17</sup> With this change the phonon structures become less pronounced. In the reflectivity spectra for the superconducting state a plasma edge appears that shifts from  $\approx 300 \text{ cm}^{-1}$  for the crystal with  $y \approx 6.9$  to  $\approx 50 \text{ cm}^{-1}$  for  $y \approx 6.6$ . For the highly underdoped crystal with  $y \approx 6.5$  the plasma edge is expected below the limit of our measurement range, i.e., for  $\omega < 30 \text{ cm}^{-1}$ . These plasma edges are due to a zero crossing of the dielectric function  $\epsilon_1(\omega) \approx -\omega_{ps}^2/\omega^2 + \epsilon_{\text{FIR}}(\omega)$ , where  $\omega_{ps}$  is the plasma frequency of the superconducting condensate and  $\epsilon_{\text{FIR}}$  the sum of high-frequency dielectric constant  $\epsilon_\infty$  and phononic contributions. This clearly indicates a change of the superconducting carrier density with doping. The reflectivity of the tetragonal crystal with  $y \approx 6.1$  is only characterized by infrared-active phonons<sup>23</sup> [Fig. 2(e)]. No additional background absorption is observable that could be caused by a small amount of free carriers and/or by inclusions of other phases as seen by Bauer *et al.*<sup>24</sup> for a crystal with  $y \approx 6.0$ . Such imperfections or finite electronic contributions cause a smearing of the appearance of phonons in the reflectivity curves, what means that the reststrahlen behavior of infrared-active phonons in insulating materials is partly lost. Almost zero reflectivity with  $\epsilon_1 \approx 1$  for longitudinal optical frequency modes is only

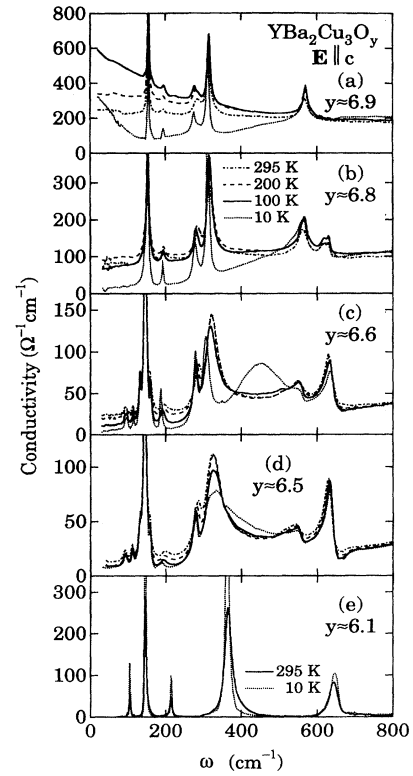


FIG. 3.  $c$ -axis conductivity of  $\text{YBa}_2\text{Cu}_3\text{O}_y$  crystals for  $y \approx 6.9$  (a), 6.8 (b), 6.6 (c), 6.5 (d) at 295 K (dash-dotted curves), 200 K (dashed), 100 K (solid), 10 K (dotted), and for  $y \approx 6.1$  (e) at 295 K (solid) and 10 K (dotted).

detectable if the absorptive part of the dielectric function is small  $\epsilon_2 \rightarrow 0$ . That is strong evidence for the purity of our crystal. This is also supported by a much higher reflectivity in the reststrahlen frequency range compared to previous results on single crystals.<sup>16,24</sup>

## B. Conductivity

For an analysis of the phonon parameters we have calculated the optical conductivity  $\sigma_1$  from the reflectivity data via a Kramers-Kronig transformation. As extrapolation towards low frequencies we used a Hagen-Rubens reflectivity  $R = 1 - \sqrt{2\omega a / \pi\sigma_0}$ , where  $\sigma_0$  is the dc conductivity, in the normal state for the conducting crystals. The reflectivity extrapolation of the insulating crystal was derived from a Lorentz oscillator fit of the experimental data. In the superconducting state the reflectivity was extrapolated within a two-fluid description regarding normal and superconductors carriers. As high-frequency extrapolation we used a  $\omega^{-4}$  decay of the reflectivity. The temperature dependence of the conductivities for the differently doped crystals are displayed in Fig. 3. For the overdoped crystal ( $y \approx 6.9$ ) the temperature variation of  $\sigma_1$  is governed by a metallic behavior of the electronic background, whereas the infrared-active phonons, which manifest in distinct narrow peaks, are only weakly influenced. With decreasing doping the electronic back-

TABLE I. Parameters of  $c$ -axis optical phonons for almost fully oxygenated, orthorhombic ( $y \approx 6.9$ ) and tetragonal  $\text{YBa}_2\text{Cu}_3\text{O}_y$  ( $y \approx 6.1$ ) at 295 and 10 K.

$\text{YBa}_2\text{Cu}_3\text{O}_y$	Symmetry	$\omega_{\text{TO}}$ ( $\text{cm}^{-1}$ )	$\gamma$ ( $\text{cm}^{-1}$ )	$S$
		295 K (10 K)	295 K (10 K)	295 K (10 K)
$y \approx 6.9$	$B_{1u}$	153(156)	6(4)	6.1(6.1)
	$B_{1u}$	194(194)	11(6)	0.4(0.6)
	$B_{1u}$	283(275)	20(11)	1(1)
	$B_{1u}$	314(312)	16(9)	2.4(2.4)
	$B_{1u}$	567(573)	22(14)	0.5(0.5)
$y \approx 6.1$	$A_{2u}$	104(104)	4(3)	1.3(1.9)
	$A_{2u}$	145(145)	6(3)	4.8(4.9)
	$A_{2u}$	213(214)	6(4)	0.4(0.5)
	$A_{2u}$	364(366)	23(9)	2.6(2.7)
	$A_{2u}$	643(645)	28(22)	0.3(0.3)

ground conductivity is reduced and an additional phonon appears above  $600 \text{ cm}^{-1}$ . For low doping ( $y \approx 6.6$  and  $6.5$ ) dramatic changes take place in the phononic part around  $320 \text{ cm}^{-1}$  with reducing temperature accompanied by growth of a broad absorption band in the vicinity of  $400 \text{ cm}^{-1}$ . Additional phonon peaks are observed below  $180 \text{ cm}^{-1}$ . For the lowest doping level ( $y \approx 6.1$ ) the conductivity is entirely determined by five infrared-active phonons [Fig. 3(e)] which exhibit almost no temperature dependence.

### C. Mode assignment

The infrared-active phonons can be assigned in the same way as reported so far.<sup>13</sup> In Table I we list the phonon parameters of all observed peaks and the mode corresponding to each peak for the two end materials with  $y \approx 6.9$  and  $6.1$ . These parameters were estimated from the conductivity spectra: the resonance frequency  $\omega_{\text{TO}}$  from the peak frequency, the damping  $\gamma$  from the half-width and the oscillator strength  $S$  from the area under the peak. The crystal symmetry of tetragonal  $\text{YBa}_2\text{Cu}_3\text{O}_6$  without Cu-O chains is represented by the space group  $D_{4h}^1$ . Group-theoretical analysis predicts five  $c$ -axis infrared-active modes with  $A_{2u}$  symmetry<sup>13</sup> which can be clearly identified in the reflectivity of the crystal with  $y \approx 6.1$ . The two low-frequency modes at 104 and  $145 \text{ cm}^{-1}$  are assigned to an out-of-phase displacement of Ba against the in-plane Cu(2) and to the vibration of Ba against Cu(1), respectively. The mode at  $213 \text{ cm}^{-1}$  represents the Y vibration and the mode at  $364 \text{ cm}^{-1}$ , which exhibits a reststrahlen behavior indicating a large  $\omega_{\text{TO}} - \omega_{\text{LO}}$  splitting, i.e., large oscillator strength, is related to the in-plane oxygen O(2) and Cu(2) bending vibration. The highest-frequency mode at  $643 \text{ cm}^{-1}$  is usually ascribed to the apical oxygen O(4) vibration.

For fully oxygenated  $\text{YBa}_2\text{Cu}_3\text{O}_7$  with  $D_{2h}^1$  symmetry seven  $c$ -axis polarized transversal optical phonons with  $B_{1u}$  symmetry are expected. Usually only five modes are observed in the infrared data because of the almost silent character of the O(2)-O(3) out-of-phase vibration and the screening of the lowest Ba mode by free carriers.

For intermediate doping, the phonon structure above  $550 \text{ cm}^{-1}$  becomes more complicated. Although a single resonance is observed for the highly doped crystal ( $y \approx 6.9$ ) with

$\omega_{\text{TO}} \approx 567 \text{ cm}^{-1}$  and for the tetragonal crystal ( $y \approx 6.1$ ) with  $\omega_{\text{TO}} \approx 643 \text{ cm}^{-1}$  it is not a gradual hardening of the apical oxygen vibration. Instead a splitting occurs presumably due to three kinds of Cu(1)-sites with two-, three-, and fourfold oxygen coordination. With reducing doping the apical oxygen O(4) moves closer to the chain copper Cu(1) and its distance to the plane copper Cu(2) increases.<sup>25</sup> With this change the apical oxygen moves in a potential that is more and more determined by the overlap of the Cu(1)  $d_{3z^2-1}$  and O(4)  $p_z$  wave functions and therefore the oxygen coordination of the Cu(1) becomes important. Notably, the corresponding O(4)-Raman line also has different positions for different Cu(1) coordinations.<sup>26</sup> As seen in Figs. 2 and 3, with reducing doping the apical oxygen mode shifts from  $567 \text{ cm}^{-1}$  down to  $552 \text{ cm}^{-1}$  for  $y \approx 6.5$ . Simultaneously, the strength of this mode decreases, which can be explained by a decrease of the density of the fourfolded Cu(1). Therefore, this mode should not be observable for the oxygen-depleted crystal with  $y \approx 6.1$ , confirmed by the experimental data in Figs. 2 and 3. On the other hand, the mode with  $\omega_{\text{TO}} \approx 630 \text{ cm}^{-1}$  seems to increase its resonance frequency up to  $643 \text{ cm}^{-1}$  for  $y \approx 6.1$  accompanied by an increasing strength consistent with an increase of the density of two-folded Cu(1). For the almost optimally doped crystal with  $y \approx 6.8$  a double-peak structure can be clearly resolved in the conductivity, indicating that this high-frequency resonance is composed by two modes possibly related to a vibration of O(4) against two- and threefold oxygen coordinated Cu(1). The gradual frequency shift of the apical oxygen modes at  $567$  and  $630 \text{ cm}^{-1}$  indicate that the crystals with intermediate dopings should not be regarded as simple multiphase systems.

For the crystal with  $y \approx 6.6$  and  $6.5$  a splitting of several phonon modes is observed at low frequencies related to the Ba displacements. It might be caused by a doubling of the unit cell along the  $a$  direction forming the orthorhombic II structure that consists of alternating empty and full chains. The strong Ba mode at  $153 \text{ cm}^{-1}$  ( $y \approx 6.9$ ) shifts with reducing oxygen content towards lower frequencies,  $145 \text{ cm}^{-1}$  for  $y \approx 6.5$  and  $6.1$ . For the in-plane oxygen bending mode the doping dependence is opposite. The resonance frequency increases from  $314 \text{ cm}^{-1}$  ( $y \approx 6.9$ ) to  $323 \text{ cm}^{-1}$  ( $y \approx 6.5$ ) ac-

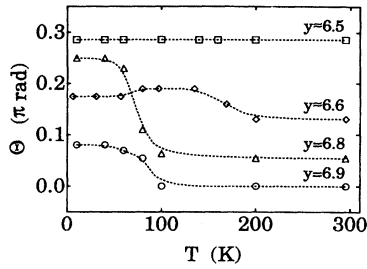


FIG. 4. Asymmetry factor  $\Theta$  for the line shape of the apical oxygen mode around  $550\text{--}570\text{ cm}^{-1}$  for different doping levels. For the crystal with  $y \approx 6.1$  only symmetric line shapes are observed,  $\Theta = 0$ .

companied by a strong increase of its linewidth. For the tetragonal crystal a much higher resonance frequency of  $364\text{ cm}^{-1}$  is found but a very narrow linewidth.

#### D. Oscillator fit for asymmetric phonons

Some of the phonon modes exhibit an asymmetric line shape, as seen in Fig. 3, presumably resulting from an interaction of these modes with the electronic background. In this case, the determination of the phonon parameters ( $\omega_{\text{TO}}$ ,  $S$ , and  $\gamma$ ) is not obvious. The method used for symmetric line shapes in the previous subsection can hardly be applied to asymmetric ones due to ambiguous estimation of the strength, for example. On the other hand, Fano line shapes can be applied for the description of the asymmetric modes but not for symmetric ones. In order to get information about the phonon parameters of the different modes we describe a phonon resonance by a Lorentz oscillator modified by a factor  $e^{i\Theta}$  where  $\Theta$  accounts for the asymmetry and take into consideration the electronic background  $\sigma_{bg}$ . The conductivity may then be written as

$$\sigma = \sigma_1 + i\sigma_2 = \frac{1}{4\pi} \frac{S\omega\omega_{\text{TO}}^2}{\gamma\omega + i(\omega_{\text{TO}}^2 - \omega^2)} e^{i\Theta} + \sigma_{bg}.$$

Similar analysis of the infrared-active phonon modes in  $\text{Pb}_2\text{Sr}_2\text{RCu}_3\text{O}_8$  was performed by Reedyk *et al.*,<sup>27</sup> who find that the asymmetry for the apical oxygen mode increases with increasing doping due to substitution of rare-earth elements  $R$ . The counterpart of this mode in highly doped  $\text{YBa}_2\text{Cu}_3\text{O}_y$  has a resonance frequency of  $567\text{ cm}^{-1}$ . We found, however, that for the crystal with the highest electronic conductivity ( $y \approx 6.9$ ) the phonon mode at  $567\text{ cm}^{-1}$  is symmetric ( $\Theta \approx 0$ ) in the normal state and shows only a small asymmetry below  $T_c$  (Fig. 4). All other modes have Lorentzian line shapes. Interestingly, with decreasing doping the apical oxygen mode becomes asymmetric already in the normal state and reaches  $\Theta \approx 0.3$  (in units of radiant  $\pi$ ) for  $y \approx 6.5$ . Similar doping and temperature dependences of  $\Theta$  are observed for the modes above  $600\text{ cm}^{-1}$  for the crystals with oxygen content  $6.5 \leq y \leq 6.8$ . In addition, for intermediate doping the in-plane oxygen mode around  $320\text{ cm}^{-1}$  exhibits a small asymmetry that is only weakly temperature dependent. Symmetric line shapes are found for the crystal with  $y \approx 6.1$  indicating no interferences with other excitations. Notably, asymmetric line shapes for infrared-active

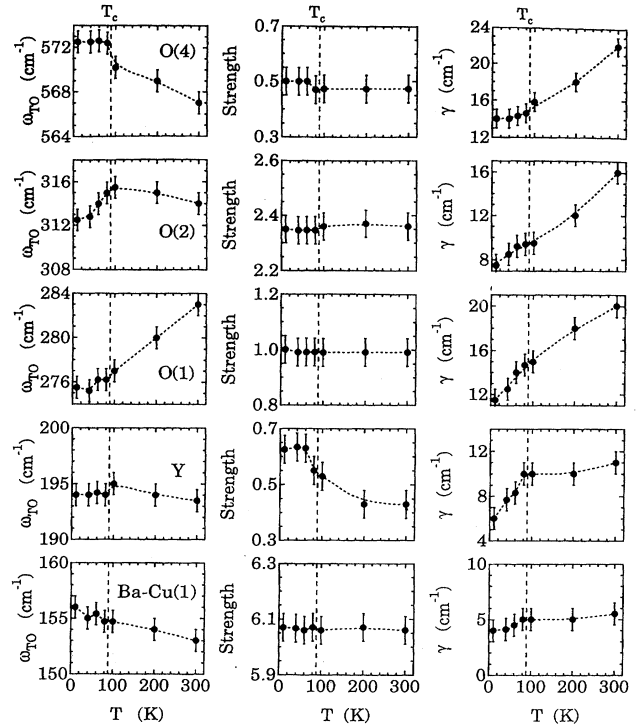


FIG. 5. Temperature dependence of resonance frequency  $\omega_{\text{TO}}$ , oscillator strength  $S$  and linewidth  $\gamma$  of *c*-axis infrared-active phonons for overdoped  $\text{YBa}_2\text{Cu}_3\text{O}_y$  ( $y \approx 6.9$ ).

phonon modes are only reported for single crystals, e.g., by Homes *et al.*<sup>4</sup> for the 60-K phase of  $\text{YBa}_2\text{Cu}_3\text{O}_y$  and by Basov *et al.*<sup>5</sup> for oxygen related modes in  $\text{YBa}_2\text{Cu}_4\text{O}_8$ , but they are usually not observed for ceramic samples.

## IV. DISCUSSION

### A. Anomalies at $T_c$

Next, based on the temperature and doping variation of the phonon parameters which were estimated by a modified Lorentzian fit and plotted in Figs. 5–8, we will discuss self-energy effects of infrared-active phonons. Changes in the real and imaginary parts of the self-energy, i.e., changes in resonance frequency and linewidth, are related to a modification of the Fermi surface, which can be caused, for example, by opening of a superconducting energy gap, if the phonon of interest couples to the electronic system. For symmetry reasons the electron-phonon coupling for odd infrared-active modes should be negligible in a one-electron band picture. Self-energy effects should be observable for even Raman modes, where a broadening is expected for modes with resonance frequencies higher than the gap due to opening of an additional decay channel.<sup>28</sup> The effects of the real part should manifest in a softening of modes lying below the gap and in a hardening for those with resonance frequencies above the gap. First application of the phonon-self energy picture for infrared-active phonons was reported by Litvinchuk *et al.*<sup>11</sup> From a comparison of results for infrared-active phonons in ceramic samples, which show strong anomalies

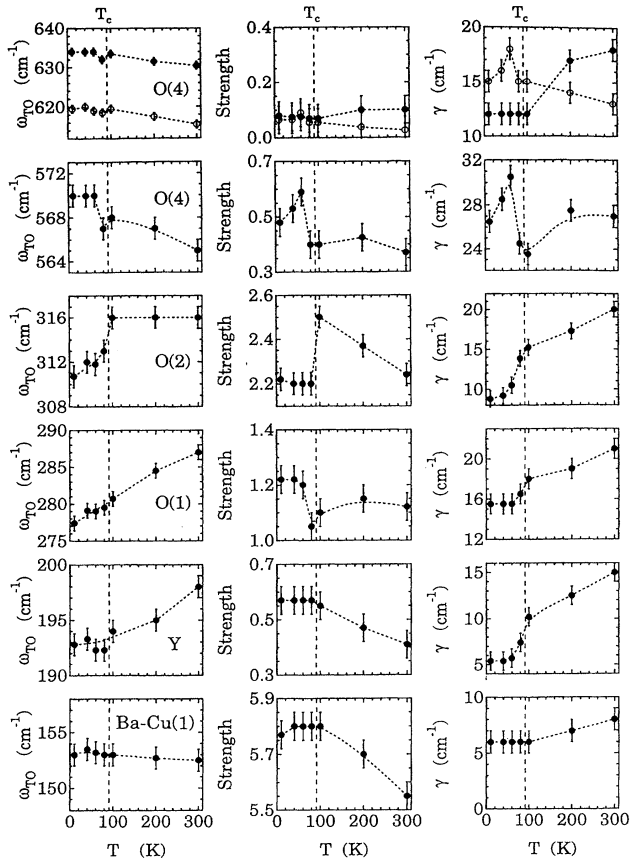


FIG. 6. Temperature dependence of resonance frequency  $\omega_{TO}$ , oscillator strength  $S$ , and linewidth  $\gamma$  of  $c$ -axis infrared-active phonons for almost optimally doped  $\text{YBa}_2\text{Cu}_3\text{O}_y$  ( $y \approx 6.8$ ).

at  $T_c$ , with Raman data a superconducting gap of  $316 \text{ cm}^{-1}$  was concluded. They found hardening of the lowest frequency mode in  $R\text{Ba}_2\text{Cu}_3\text{O}_y$  for  $R=\text{Tm}$ , softening of the four modes at higher frequencies for  $R=\text{Tm}$ , Er and broadening of the apical oxygen mode, in agreement with results for ceramic  $\text{YBa}_2\text{Cu}_3\text{O}_y$  with  $y \approx 7$ .

For our almost fully oxygenated crystal, the temperature dependences of the phonon modes apparently differ from those of ceramic samples (Fig. 5). The only mode which exhibits a substantial change in its resonance frequency at  $T_c$  is the in-plane oxygen bending mode, all other remain essentially uninfluenced at  $T_c$ . The frequency shift of  $\Delta\omega/\omega \approx 1\%$  for the in-plane oxygen mode is in agreement with data of polycrystalline  $\text{YBa}_2\text{Cu}_3\text{O}_7$  in Ref. 10, but twice as high as the results of inelastic neutron scattering for  $\text{YBa}_2\text{Cu}_3\text{O}_{6.92}$ .<sup>29</sup> Furthermore, we find no remarkable change in the  $T$  dependences of the linewidths for all modes, except for the  $Y$  vibration at  $194 \text{ cm}^{-1}$ .

Also the magnitudes of strengths obtained for single crystals coincide with calculated values<sup>13</sup> and have a reasonable contribution of  $\sum S_i \approx 10$  to the static dielectric constant, in contrast to polycrystalline material where oscillator strengths of 20 for the Ba mode were found.<sup>3</sup> The lack of superconductivity related effects on the phonon self-energy of the  $B_{1u}$  modes for fully oxygenated  $\text{YBa}_2\text{Cu}_3\text{O}_y$  can be explained by symmetry considerations. Hence, in the simplest

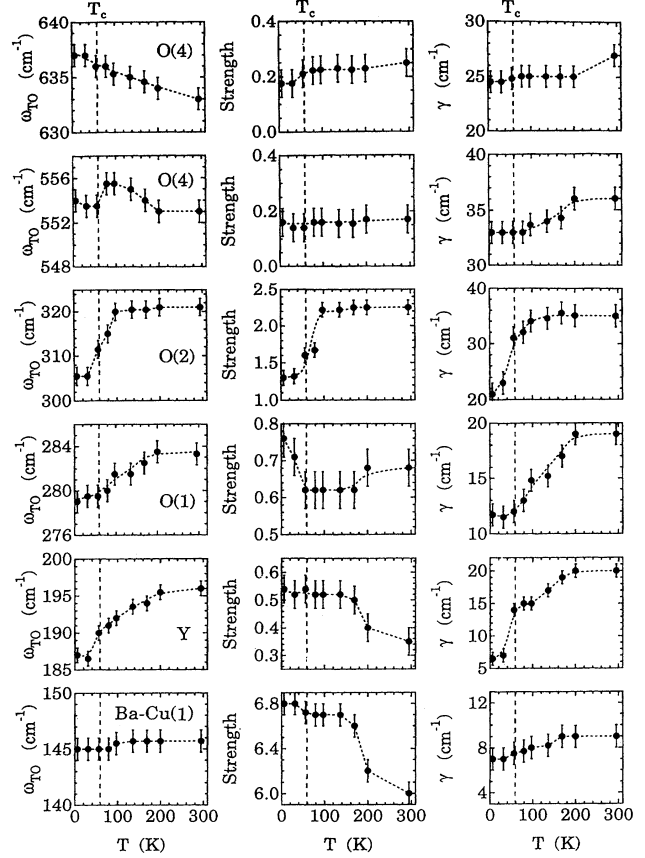


FIG. 7. Temperature dependence of resonance frequency  $\omega_{TO}$ , oscillator strength  $S$ , and linewidth  $\gamma$  of  $c$ -axis infrared-active phonons for underdoped  $\text{YBa}_2\text{Cu}_3\text{O}_y$  ( $y \approx 6.6$ ).

approximation, odd phonons should not couple to excitations of quasiparticles across the superconducting gap. Raman measurements, performed on the same crystal, showed no Raman forbidden modes<sup>30</sup> which are usually ascribed either to impurities or disorder due to oxygen vacancies.<sup>31</sup> This strongly supports that our overdoped crystal is highly stoichiometric and has a perfect crystal structure that might be the origin for a negligible coupling of the odd  $q=0$  phonons with the electronic background.

To describe the softening of the in-plane oxygen mode, it is suggested that the buckling of the  $\text{CuO}_2$  planes could provide a sufficient coupling of odd oxygen vibrations to spin variables via an effective modulation of the superexchange interaction  $J$  between Cu.<sup>32</sup> However, the calculation of a frequency shift of the oxygen bending mode for a single layer model predicts an almost negligible value. The strong softening of this mode seems to be inconsistent with such single layer models and may indicate that this effect is driven by a coupling of the mode to charge fluctuations between adjacent  $\text{CuO}_2$  layers. Considering a symmetric and an anti-symmetric electronic plane-band crossing the Fermi energy, an odd infrared-active phonon with energy similar to the band splitting energy can couple to such interband transitions. Therefore, the opening of a superconducting gap should have strong influence on the phonon self energies as proposed by Hastreiter *et al.*<sup>2</sup> The only modes which show a

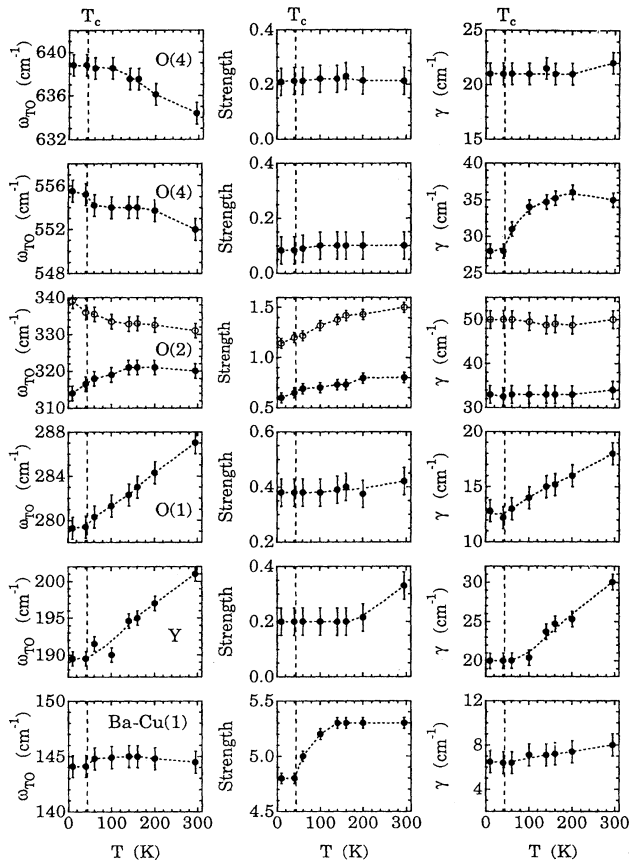


FIG. 8. Temperature dependence of resonance frequency  $\omega_{TO}$ , oscillator strength  $S$ , and linewidth  $\gamma$  of  $c$ -axis infrared-active phonons for highly underdoped  $\text{YBa}_2\text{Cu}_3\text{O}_y$  ( $y \approx 6.5$ ).

change in their self-energies at  $T_c$  are related to the in-plane oxygen vibration with Y displacement between adjacent  $\text{CuO}_2$  planes that may support the picture above. Notably, the chain oxygen vibration at  $283 \text{ cm}^{-1}$ , that exhibits the strongest temperature variation in the normal state, is found to be substantially unchanged at  $T_c$ .

For the optimally doped crystal with  $y \approx 6.8$  pronounced changes in the imaginary part of phonon self-energies take place at the superconducting transition, as shown in Fig. 6. The linewidth of three modes with resonance frequencies lower than  $320 \text{ cm}^{-1}$  narrows more strongly below  $T_c$ , whereas it maintains constant for the lowest-frequency mode. The apical oxygen vibration at  $556 \text{ cm}^{-1}$  exhibits a broadening just below  $T_c$  and narrows again for  $T < 60 \text{ K}$ . Similar behavior is observed for the  $620 \text{ cm}^{-1}$  mode but not for that at  $635 \text{ cm}^{-1}$ . Clear changes in the oscillator strength for the oxygen related modes occur at  $T_c$ . A sudden drop of  $S$  for the in-plane bending mode should be emphasized which is in strong contrast to an enhancement of  $S$ , usually found in polycrystalline material.<sup>10,11</sup> Only this mode exhibits a softening below  $T_c$ , similar to that observed for the fully oxygenated crystal with a drop of approximately  $5 \text{ cm}^{-1}$  between  $T_c$  and  $10 \text{ K}$ . Moreover, its damping is strongly reduced below  $T_c$ .

In this crystal the translation symmetry is partly lost due to a certain amount of disorder in the oxygen sublattice. In

this case, simple symmetry considerations are no longer valid. Therefore, superconductivity related self-energy effects of the infrared phonons could explain the changes in the linewidth of several phonons for our almost optimally doped  $\text{YBa}_2\text{Cu}_3\text{O}_y$  crystal with  $y \approx 6.8$ . A decrease of damping due to opening of a superconducting gap should be observable if the lifetime of phonons in the normal state is partly determined by scattering at quasiparticles. Although  $k$ -vector selection rules normally forbid a creation of an electron-hole pair by a  $q=0$  phonon, the weak asymmetry of the modes indicate a coupling with the electronic background. Therefore, phonons with energies smaller than the gap or in the energy region with reduced density of quasiparticle states may lose a decay channel manifesting in a narrowing of the phonon peak. On the other hand, phonons with higher energies broaden due to the possibility of breaking a superconducting pair.

The linewidths of the modes above  $550 \text{ cm}^{-1}$  show a very interesting temperature dependence below  $T_c$  (see Fig. 6), which might be associated with the temperature variation of an superconducting gap. The broadening just below  $T_c$  of the  $565$  and  $620 \text{ cm}^{-1}$  mode followed by a narrowing below  $60 \text{ K}$  could indicate that the gap is smaller than  $565 \text{ cm}^{-1}$  above  $60 \text{ K}$  and larger than  $620 \text{ cm}^{-1}$  below  $60 \text{ K}$ . Since a light broadening is observed for the  $630 \text{ cm}^{-1}$  mode, it is possible to estimate an upper limit for the maximum gap amplitude of  $620 \text{ cm}^{-1}$ . The superconductivity related suppression of the electronic background conductivity exhibits similar features, the onset of the suppression is approximately  $500 \text{ cm}^{-1}$  just below  $T_c$  and  $600 \text{ cm}^{-1}$  for  $T \ll T_c$ .<sup>33</sup> This behavior is consistent with  $d$ -wave pairing, because calculations for such type of superconductivity show that the onset of suppression roughly coincides with the maximum energy  $2\Delta_0$  of the gap distribution.<sup>34</sup> For the underdoped crystals almost no change in the phonon parameters is observed at  $T_c$  (Figs. 7 and 8). Instead a remarkable change appears well above  $T_c$ , as described below.

## B. Anomalies in the normal state

Two characteristic features determine the conductivity of the underdoped crystals with  $y \approx 6.6$  and  $6.5$ , that is displayed in Fig. 3. One is a growing absorption band in the vicinity of  $450$  and  $400 \text{ cm}^{-1}$  with reducing temperature, the other is the strong temperature dependence of the oxygen bending mode at  $320 \text{ cm}^{-1}$  that is apparently different for the two doping levels. It narrows for the crystal with  $y \approx 6.6$  with decreasing temperature and strongly broadens for  $y \approx 6.5$ . Another difference is that this phonon peak for  $y \approx 6.6$  can be described by a slightly asymmetric Lorentzian lineshape, whereas a single resonance fails in the case of  $y \approx 6.5$ , especially at low temperature ( $10 \text{ K}$ ) and it seems to be composed of two different resonances. The appearance of two modes could originate from a separation of the tetragonal and orthorhombic phase for such low oxygen concentrations. Notably, the resonance frequency of the oxygen bending is approximately  $40 \text{ cm}^{-1}$  higher for the tetragonal phase than for the orthorhombic phase.

Taking into account three resonances for  $y \approx 6.5$ , the best fits of the phonon peaks at  $280$  and  $320 \text{ cm}^{-1}$ , are shown in Figs. 9(a)–9(f) at three different temperatures (dotted

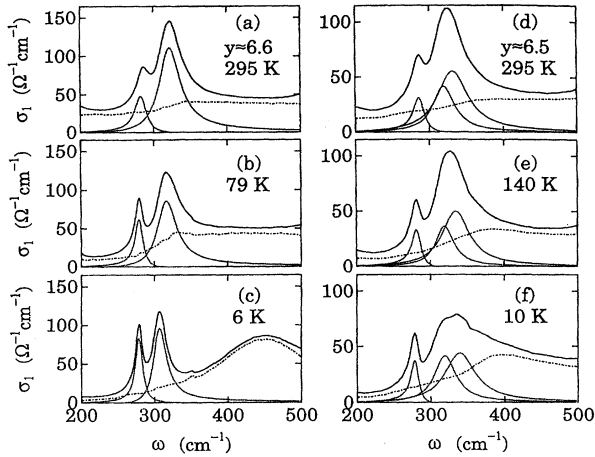


FIG. 9.  $c$ -axis conductivity of underdoped  $\text{YBa}_2\text{Cu}_3\text{O}_y$  with  $y \approx 6.6$  for 295 K (a), 79 K (b), and 6 K (c) and  $y = 6.5$  for 295 K (d), 140 K (e), and 10 K (f) in the vicinity of the in-plane oxygen bending mode. The dotted lines show a fit of the phonon modes. The dash-dotted line represents the remaining background conductivity after subtracting the phononic contribution. The spectral weight of the oxygen bending modes strongly decreases with temperature and is partly transferred to a broad absorption bands centered around  $450 \text{ cm}^{-1}$  for  $y \approx 6.6$  and  $400 \text{ cm}^{-1}$  for  $y \approx 6.5$ .

curves). After subtracting the phononic part from the experimental data the residual conductivity is displayed as dash-dotted curves in Fig. 9. With reducing temperature the residual conductivity decreases below  $300 \text{ cm}^{-1}$  for both crystals. Above  $400 \text{ cm}^{-1}$  a strong increase of spectral weight occurs at a specific temperature for the two doping levels. The increase is observed below 100 K for the crystal with  $y \approx 6.6$  and below 160 K for  $y \approx 6.5$ . The appearance of this anomaly is accompanied by a decrease of the strength of the in-plane oxygen bending mode that sets in at almost the same temperature indicating that the spectral weight is partly transferred from the in-plane oxygen bending mode to the broad absorption band around  $400 \text{ cm}^{-1}$  and thus this absorption band might have a phononic origin.

The detailed temperature dependence of all phonon parameters is shown in Figs. 7 and 8. There occur pronounced anomalies in the normal state. For  $y \approx 6.6$  the resonance frequency, strength, and linewidth of the in-plane oxygen bending mode start to decrease dramatically approximately 40 K above  $T_c$  with a relative change  $\Delta\omega_{\text{TO}}/\omega_{\text{TO}} \approx 4\%$  and  $\Delta S/S \approx 40\%$  between 100 and 6 K. An anomaly at  $T_c$  is only an increase of the strength for the chain oxygen vibration.

For lower oxygen content  $y \approx 6.5$  the in-plane oxygen bending mode seems to be composed of two modes. From a comparison of the resonance frequencies for the different doping levels, the mode at lower frequency ( $320 \text{ cm}^{-1}$ ) might be associated with the orthorhombic phase. This mode exhibits a similar temperature dependence compared with that for  $y \approx 6.6$ , but the softening occurs at a higher temperature  $\approx 160 \text{ K}$  (Fig. 9). The mode at higher frequencies ( $330 \text{ cm}^{-1}$ ) hardens below this temperature which explains the broadening of the peak in the conductivity. The total strength of these modes starts to drop already below 295 K but is more pronounced below 160 K which is independent on the

description of the peak in the conductivity. In addition the strength of the Ba mode decreases and the linewidth of the apical oxygen mode at  $552 \text{ cm}^{-1}$  narrows below this temperature. The other modes remain unchanged and no anomalies at  $T_c$  are observed.

In contrast to the two underdoped crystals, the five phonon modes of the tetragonal crystal with lowest oxygen content ( $y \approx 6.1$ ) show only a gradual narrowing as well as an increase of the strength of the Ba mode as seen in Table I. The other phonon parameters exhibit no temperature dependence.

For the 60-K phase of  $\text{YBa}_2\text{Cu}_3\text{O}_y$  ( $y \approx 6.6-6.7$ ) frequency shifts for polycrystalline samples are reported to occur clearly above  $T_c$  ( $\approx 150 \text{ K}$ ) and for the lightly underdoped  $\text{YBa}_2\text{Cu}_4\text{O}_8$  at  $\approx 120 \text{ K}$ .<sup>35</sup> These features were discussed in connection with the onset temperature of a spin gap which was suggested by the maximum of the nuclear relaxation rate  $(TT_1)^{-1}$  observed at  $T_0 \approx 150 \text{ K}$ .<sup>36,37</sup> However, it is questionable whether all phonon anomalies above  $T_c$  indicate a direct coupling of phonons to the spin system. Because infrared-active phonons cause a change in the electrical dipole moment, they primarily couple to charge excitations. As we reported in separate papers,<sup>6</sup> for underdoped crystals a conductivity suppression below a characteristic frequency sets in well above  $T_c$ , being consistent with a semiconducting behavior of the dc conductivity, and no dramatic change is observed at  $T_c$ . This suppression can be caused by a pseudogap opening in the charge excitation spectrum along the  $c$  direction. The observed changes above  $T_c$  in the self-energy of the in-plane oxygen bending mode for the underdoped crystals with  $y \approx 6.6$  and  $6.5$  could be associated with this change in the electronic system, which might be strongly influenced by spin variables.

The origin of the growing bump around  $400 \text{ cm}^{-1}$  in the conductivity is not clear. The fact that the onset temperature of these anomalies coincide with the spin-gap temperature reported for  $\text{YBa}_2\text{Cu}_3\text{O}_{6.52}$  by Yasuoka *et al.*<sup>36</sup> may suggest a lattice distortion driven by the opening of a spin gap. For a deeper understanding, a precise study of the temperature dependence of the crystal structure for the underdoped compounds is necessary.

## V. CONCLUSION

We have studied the temperature dependence of infrared-active phonons with vibrations parallel to the  $c$  axis of overdoped, optimally doped, underdoped, and insulating  $\text{YBa}_2\text{Cu}_3\text{O}_y$  ( $y \approx 6.9, 6.8, 6.6, 6.5,$  and  $6.1$ ) single crystals by measuring the infrared reflectivity with  $\mathbf{E} \parallel c$ . The phonon parameters (resonance frequency, oscillator strength, and linewidth) were estimated from the conductivity calculated via a Kramers-Kronig transformation of the reflectivity data. For the overdoped crystal almost no anomalies of the phonon self-energies were observed, except for a softening of the in-plane oxygen bending mode and a narrowing of the linewidth of the Y vibration at  $T_c$ . These modes may couple to charge fluctuations between adjacent  $\text{CuO}_2$  planes. Pronounced effects on the phonon self-energies for the optimally doped crystal at the superconducting transition were found, which are attributed to a lower crystal symmetry caused by disorder in the oxygen sublattice. The temperature variation

of the linewidths of the apical oxygen modes can be explained by the temperature dependence of an anisotropic superconducting gap with a maximum amplitude of  $2\Delta_0 \approx 620 \text{ cm}^{-1}$ . In the underdoped crystals the strong decrease of the resonance frequency and oscillator strength for the in-plane oxygen bending mode might be associated with the suppression of the  $c$ -axis conductivity, i.e., by a pseudogap in the charge excitations. The onset temperatures of these phenomena (phonon anomalies, conductivity suppression and spin gap opening) scale with each other and decrease with doping. Because the decrease of the oscillator strength seems to be compensated by the growth of spectral weight of a strong absorption band centered at  $450 \text{ cm}^{-1}$  for

$y \approx 6.6$  and  $400 \text{ cm}^{-1}$  for  $y \approx 6.5$ , we suggest that this absorption band represents a phononic excitation, which might originate from some lattice distortion.

#### ACKNOWLEDGMENTS

We would like to thank Y. Yamada and Y. Shiohara at the Superconductivity Research Laboratory (SRL), ISTEK for their help in sample preparation, and I. Terasaki for his help in transport measurements on our crystals. This work was partially supported by NEDO for the R&D of Industrial Science and Technology Frontier Program.

- <sup>1</sup>B. Friedl, C. Thomsen, and M. Cardona, *Phys. Rev. Lett.* **65**, 915 (1990).
- <sup>2</sup>G. Hastreiter, U. Hofmann, J. Keller, and K. F. Renk, *Solid State Commun.* **76**, 1015 (1990).
- <sup>3</sup>K. Takenaka, K. Mizuhashi, H. Takagi, and S. Uchida, *Phys. Rev. B* **50**, 6534 (1994).
- <sup>4</sup>C. C. Homes, T. Timusk, R. Liang, D. A. Bonn, and W. N. Hardy, *Phys. Rev. Lett.* **71**, 1645 (1993).
- <sup>5</sup>D. N. Basov, T. Timusk, B. Dabroski, and J. D. Jorgensen, *Phys. Rev. B* **50**, 3511 (1994).
- <sup>6</sup>S. Tajima, J. Schützmann, and S. Miyamoto, *Solid State Commun.* **95**, 759 (1995); J. Schützmann, S. Tajima, S. Miyamoto, and S. Tanaka, in *Advances in Superconductivity VII*, edited by K. Yamafuji and T. Morishita (Springer-Verlag, Tokyo, 1995), p. 161.
- <sup>7</sup>P. Nyhus, M. A. Karlow, and S. L. Cooper, *Phys. Rev. B* **50**, 13 898 (1994).
- <sup>8</sup>D. A. Bonn, A. H. O'Reilly, J. E. Greedan, C. V. Stager, T. Timusk, K. Kamarás, and D. B. Tanner, *Phys. Rev. B* **37**, 1574 (1988).
- <sup>9</sup>W. Ose, P. E. Obermayer, H. H. Otto, T. Zetterer, H. Lengfellner, J. Keller, and K. F. Renk, *Z. Phys. B* **70**, 307 (1988).
- <sup>10</sup>L. Genzel, A. Wittlin, M. Bauer, M. Cardona, E. Schönherr, and A. Simon, *Phys. Rev. B* **40**, 2170 (1989).
- <sup>11</sup>A. P. Litvinchuk, C. Thomsen, and M. Cardona, *Solid State Commun.* **80**, 257 (1991).
- <sup>12</sup>A. P. Litvinchuk, C. Thomsen, and M. Cardona, *Solid State Commun.* **83**, 343 (1992).
- <sup>13</sup>A. P. Litvinchuk, C. Thomsen, and M. Cardona, in *Physical Properties of High Temperature Superconductors IV*, edited by D. M. Ginsberg (World Scientific, Singapore, 1994).
- <sup>14</sup>M. Bauer, Ph.d. thesis, University of Tübingen.
- <sup>15</sup>B. Koch, M. Dürler, H. P. Geserich, Th. Wolf, G. Roth, and G. Zachmann, in *Electronic Properties of High- $T_c$  Superconductors and Related Compounds*, edited by H. Kuzmany, M. Mehring, and J. Fink (Springer-Verlag, Berlin, 1990), p. 290.
- <sup>16</sup>A. V. Bazhenov and V. B. Timofeev, *Physica C* **162-164**, 1247 (1989).
- <sup>17</sup>J. Schützmann, S. Tajima, S. Miyamoto, and S. Tanaka, *Phys. Rev. Lett.* **73**, 174 (1994).
- <sup>18</sup>R. T. Collins, Z. Schlesinger, F. Holtzberg, and C. Feild, *Phys. Rev. Lett.* **63**, 422 (1989).
- <sup>19</sup>Z. Schlesinger, R. T. Collins, F. Holtzberg, C. Feild, G. Koren, and A. Gupta, *Phys. Rev. B* **41**, 11 237 (1990).
- <sup>20</sup>Y. Yamada and Y. Shiohara, *Physica C* **217**, 182 (1993).
- <sup>21</sup>S. Miyamoto, Y. High, J. Schützmann, H. Kutami, Y. Yamada, S. Tajima, and S. Shiohara, in *Advances in Superconductivity VII* (Ref. 6), p. 129.
- <sup>22</sup>I. Terasaki, Y. Sato, S. Tajima, S. Miyamoto, and S. Tanaka, *Physica C* **235-240**, 1413 (1994); I. Terasaki, Y. Sato, S. Miyamoto, S. Tajima, and S. Tanaka, *Phys. Rev. B* (to be published).
- <sup>23</sup>S. Tajima, J. Schützmann, S. Miyamoto, O. V. Misochko, and S. Tanaka, *Physica C* **235-240**, 1171 (1994).
- <sup>24</sup>M. Bauer, I. B. Ferreira, L. Genzel, M. Cardona, P. Murugaraj, and J. Maier, *Solid State Commun.* **72**, 551 (1989).
- <sup>25</sup>J. D. Jorgensen, B. W. Veal, A. P. Paulikas, L. J. Nowicki, G. W. Crabtree, H. Claus, and W. K. Kwok, *Phys. Rev. B* **41**, 1863 (1990).
- <sup>26</sup>V. G. Hadjiev, C. Thomsen, J. Kircher, and M. Cardona, *Phys. Rev. B* **47**, 9148 (1993).
- <sup>27</sup>M. Reedyk, T. Timusk, J. S. Xue, and J. E. Greedan, *Phys. Rev. B* **49**, 15 984 (1994).
- <sup>28</sup>R. Zeyher and G. Zwirnagl, *Z. Phys. B* **78**, 175 (1990).
- <sup>29</sup>N. Pyka, W. Reichhardt, L. Pintschovios, G. Engel, J. Rossat-Mignod, and J. Y. Henry, *Phys. Rev. Lett.* **70**, 1457 (1993).
- <sup>30</sup>O. V. Misochko, S. Tajima, S. Miyamoto, H. Kobayashi, S. Kagiya, N. Watanabe, N. Koshizuka, and S. Tanaka, *Phys. Rev. B* **51**, 1346 (1995).
- <sup>31</sup>K. F. McCarty, J. Z. Liu, Y. X. Jia, R. N. Shelton, and H. B. Radousky, *Physica C* **192**, 331 (1992).
- <sup>32</sup>B. Normand, H. Kohno, and H. Fukuyama (unpublished).
- <sup>33</sup>J. Schützmann, S. Tajima, S. Miyamoto, Y. Sato, and I. Terasaki, *Solid State Commun.* **94**, 293 (1995).
- <sup>34</sup>M. J. Graf, M. Palumbo, D. Rainer, and J. A. Sauls (unpublished).
- <sup>35</sup>A. P. Litvinchuk, C. Thomsen, P. Murugaraj, and M. Cardona, *Z. Phys. B* **86**, 329 (1992).
- <sup>36</sup>H. Yasuoka, T. Imai, and T. Shimizu, in *Strong Correlation and Superconductivity*, edited by H. Fukuyama, S. Maekawa, and A. P. Malezemo, Springer Series in Solid State Sciences Vol. 89 (Springer-Verlag, Berlin, 1989), p. 254.
- <sup>37</sup>M. Takigawa, A. P. Reyes, P. C. Hammel, J. D. Thompson, R. H. Heffner, Z. Fisk, and K. C. Ott, *Phys. Rev. B* **43**, 247 (1991).